

Quantum discord for two-qubit X states

Mazhar Ali,^{1,3,*} A. R. P. Rau,² and G. Alber¹

¹*Institut für Angewandte Physik, Technische Universität Darmstadt, Darmstadt D-64289, Germany*

²*Department of Physics and Astronomy, Louisiana State University, Baton Rouge, Louisiana 70803, USA*

³*Department of Electrical Engineering, COMSATS Institute of Information Technology, Abbottabad 22060, Pakistan*

(Received 18 February 2010; published 12 April 2010)

Quantum discord, a kind of quantum correlation, is defined as the difference between quantum mutual information and classical correlation in a bipartite system. In general, this correlation is different from entanglement, and quantum discord may be nonzero even for certain separable states. Even in the simple case of bipartite quantum systems, this different kind of quantum correlation has interesting and significant applications in quantum information processing. So far, quantum discord has been calculated explicitly only for a rather limited set of two-qubit quantum states and expressions for more general quantum states are not known. In this article, we derive explicit expressions for quantum discord for a larger class of two-qubit states, namely, a seven-parameter family of so called X states that have been of interest in a variety of contexts in the field. We also study the relation between quantum discord, classical correlation, and entanglement for a number of two-qubit states to demonstrate that they are independent measures of correlation with no simple relative ordering between them.

DOI: [10.1103/PhysRevA.81.042105](https://doi.org/10.1103/PhysRevA.81.042105)

PACS number(s): 03.65.Ta, 03.67.—a

I. INTRODUCTION

For a given bipartite quantum state, it is important to know whether it is entangled, separable, classically correlated, or quantum correlated. Much effort has been invested in subdividing quantum states into separable and entangled states (see Refs. [1,2] and references therein). It is well known that entanglement makes possible tasks in quantum information which are impossible without it [3]. However, entanglement is not the only type of correlation useful for quantum technology. Recently, it was found that there are some quantum correlations other than entanglement that also offer some advantage, for example, quantum nonlocality without entanglement [4–6]. In addition, it was shown theoretically [7–9], and later experimentally [10], that some separable states may also speed up certain tasks over their classical counterparts. Therefore, it is desirable to investigate, characterize, and quantify quantum correlations more broadly.

A bipartite quantum state contains both classical and quantum correlations. These correlations are quantified jointly by their “quantum mutual information,” an information-theoretic measure of the total correlation in a bipartite quantum state [11]. In particular, if ρ^{AB} denotes the density operator of a composite bipartite system AB and $\rho^A(\rho^B)$ denotes the density operator of part $A(B)$, then the quantum mutual information is defined as

$$\mathcal{I}(\rho^{AB}) = S(\rho^A) + S(\rho^B) - S(\rho^{AB}), \quad (1)$$

where $S(\rho) = -\text{tr}(\rho \log_2 \rho)$ is the von Neumann entropy. Moreover, it was shown that quantum mutual information is the maximum amount of information that A(lice) can send securely to B(ob) if a composite correlated quantum state is used as the key for a *one-time pad cryptographic system* [12].

Quantum mutual information may be written as a sum of classical correlation $\mathcal{C}(\rho^{AB})$ and quantum correlation

$\mathcal{Q}(\rho^{AB})$, that is, $\mathcal{I}(\rho^{AB}) = \mathcal{C}(\rho^{AB}) + \mathcal{Q}(\rho^{AB})$ [13–15]. This quantum part \mathcal{Q} has been called quantum discord [13]. It is a different type of quantum correlation than entanglement because separable mixed states (that is, with no entanglement) can have nonzero quantum discord.

Quantum discord is not always larger than entanglement [15,16]. This indicates that discord is not simply a sum of entanglement and some other nonclassical correlation. Even for the simplest case of two entangled qubits, the relation between quantum discord, entanglement, and classical correlation is not yet clear. For pure states and, surprisingly, for a mixture of Bell states, quantum correlation is exactly equal to entanglement, whereas classical correlation attains its maximum value 1. However, for general two-qubit mixed states, the situation is more complicated. Qubit-qubit entanglement has been characterized and quantified completely, whereas quantum discord has been characterized and quantified only for particular cases [13–20]. More recently, some analytical results were obtained for a restricted subset of two-qubit X states with an interest in the dynamics of quantum discord [21,22]. Another measure called “quantumness of correlations” is introduced as well, which has the property that it vanishes for separable states [23]. Quantum discord is a measure of nonclassical correlations that may include entanglement but is an independent measure. We document with simple examples that the amounts of classical correlation, quantum discord, and entanglement bear no simple relationship to each other.

In order to quantify quantum discord, Ollivier and Zurek [13] suggested the use of von Neumann type measurements which consist of one-dimensional projectors that sum to the identity operator. Let the projection operators $\{B_k\}$ describe a von Neumann measurement for subsystem B only, then the conditional density operator ρ_k associated with the measurement result k is

$$\rho_k = \frac{1}{p_k} (I \otimes B_k) \rho (I \otimes B_k), \quad (2)$$

*mazharaliawan@yahoo.com

where the probability p_k equals $\text{tr}[(I \otimes B_k)\rho(I \otimes B_k)]$. The quantum conditional entropy with respect to this measurement is given by [15]

$$S(\rho|\{B_k\}) := \sum_k p_k S(\rho_k), \quad (3)$$

and the associated quantum mutual information of this measurement is defined as

$$\mathcal{I}(\rho|\{B_k\}) := S(\rho^A) - S(\rho|\{B_k\}). \quad (4)$$

A measure of the resulting classical correlations is provided [13–16] by

$$\mathcal{C}(\rho) := \sup_{\{B_k\}} \mathcal{I}(\rho|\{B_k\}). \quad (5)$$

The obstacle to computing quantum discord lies in this complicated maximization procedure for calculating the classical correlation because the maximization is to be done over all possible von Neumann measurements of B . Once \mathcal{C} is in hand, quantum discord is simply obtained by subtracting it from the quantum mutual information,

$$\mathcal{Q}(\rho) := \mathcal{I}(\rho) - \mathcal{C}(\rho). \quad (6)$$

For a general two-qubit X state, the quantification of quantum discord is still missing, with only partial results available for subsets of three parameters [15,19,20] and some other restricted subsets of two-qubit X states [21,22,24].

Therefore, in order to deepen our understanding of quantum discord and its relation to other forms of quantum correlations such as entanglement, it is necessary to generalize these first results and develop methods for computing quantum discord in more general contexts. In this article, we develop such a method to evaluate both classical correlations and quantum discord for the complete set of two-qubit X states depending on seven real-valued parameters. Among others, this set includes maximally entangled Bell states and separable and nonseparable ‘‘Werner’’ states [25]. Analytical expressions are derived which explicitly exhibit the dependence of classical correlation and quantum discord on the density matrix elements of arbitrary X states. It is demonstrated that already within this seven-parameter set of states, there are no simple ordering relations between entanglement and discord. Thus, these analytical results strongly support the general view that entanglement and discord are two fundamentally different types of quantum correlations.

This article is organized as follows. In Sec. II, we describe some basic properties of X states and how to calculate the classical correlation and quantum discord for them. In Sec. III, we apply this for various examples of X states, studying the relation between the classical correlation, quantum discord, and entanglement. We conclude our work in Sec. IV. In the Appendix we present details while extending also the calculation from von Neumann measurements to more general positive operator valued measurements (POVM) of one subsystem.

II. TWO-QUBIT X STATES

In this section, we limit our discussion to initially prepared arbitrary two-qubit X states. The density matrix of a two-

qubit X state in the representation spanned by the two-qubit product states $|1\rangle = |0\rangle_A \otimes |0\rangle_B$, $|2\rangle = |0\rangle_A \otimes |1\rangle_B$, $|3\rangle = |1\rangle_A \otimes |0\rangle_B$, and $|4\rangle = |1\rangle_A \otimes |1\rangle_B$ is of the general form

$$\rho_X = \begin{pmatrix} \rho_{11} & 0 & 0 & \rho_{14} \\ 0 & \rho_{22} & \rho_{23} & 0 \\ 0 & \rho_{32} & \rho_{33} & 0 \\ \rho_{41} & 0 & 0 & \rho_{44} \end{pmatrix}, \quad (7)$$

that is, $\rho_{12} = \rho_{13} = \rho_{24} = \rho_{34} = 0$. This visual appearance resembling the letter X has led them to be called X states [26] but, recently, an underlying symmetry structure of these states has been examined [27].

Equation (7) describes a quantum state provided the unit trace and positivity conditions $\sum_{i=1}^4 \rho_{ii} = 1$, $\rho_{22}\rho_{33} \geq |\rho_{23}|^2$, and $\rho_{11}\rho_{44} \geq |\rho_{14}|^2$ are fulfilled. X states are entangled if and only if either $\rho_{22}\rho_{33} < |\rho_{23}|^2$ or $\rho_{11}\rho_{44} < |\rho_{14}|^2$. Both conditions cannot hold simultaneously [28]. Equation (7) is a seven-real parameter state with three real parameters along the main diagonal and two complex (or four real) parameters at off-diagonal positions.

The eigenvalues of the density matrix ρ_X in Eq. (7) are given by

$$\begin{aligned} \lambda_0 &= \frac{1}{2} [(\rho_{11} + \rho_{44}) + \sqrt{(\rho_{11} - \rho_{44})^2 + 4|\rho_{14}|^2}], \\ \lambda_1 &= \frac{1}{2} [(\rho_{11} + \rho_{44}) - \sqrt{(\rho_{11} - \rho_{44})^2 + 4|\rho_{14}|^2}], \\ \lambda_2 &= \frac{1}{2} [(\rho_{22} + \rho_{33}) + \sqrt{(\rho_{22} - \rho_{33})^2 + 4|\rho_{23}|^2}], \\ \lambda_3 &= \frac{1}{2} [(\rho_{22} + \rho_{33}) - \sqrt{(\rho_{22} - \rho_{33})^2 + 4|\rho_{23}|^2}]. \end{aligned} \quad (8)$$

The quantum mutual information is given as

$$\mathcal{I}(\rho_X) = S(\rho_X^A) + S(\rho_X^B) + \sum_{j=0}^3 \lambda_j \log_2 \lambda_j, \quad (9)$$

where ρ_X^A and ρ_X^B are the marginal states of ρ_X , and

$$\begin{aligned} S(\rho_X^A) &= -[(\rho_{11} + \rho_{22}) \log_2(\rho_{11} + \rho_{22}) \\ &\quad + (\rho_{33} + \rho_{44}) \log_2(\rho_{33} + \rho_{44})], \\ S(\rho_X^B) &= -[(\rho_{11} + \rho_{33}) \log_2(\rho_{11} + \rho_{33}) \\ &\quad + (\rho_{22} + \rho_{44}) \log_2(\rho_{22} + \rho_{44})]. \end{aligned} \quad (10)$$

After computing the quantum mutual information, we need next to compute the classical correlation $\mathcal{C}(\rho_X)$. We consider projective measurements for subsystem B (the projective measurements for subsystem A give the same results if we restrict to either $\rho_{11} = \rho_{44}$ or $\rho_{22} = \rho_{33}$). We follow the procedure of [15] except that we are considering a class of states that is more general than the three-parameter family of that study.

It is known that any von Neumann measurement for subsystem B can be written as Ref. [15]

$$B_i = V \Pi_i V^\dagger, \quad i = 0, 1, \quad (11)$$

where $\Pi_i = |i\rangle\langle i|$ is the projector for subsystem B along the computational base $|i\rangle$ and $V \in SU(2)$ is a unitary operator with unit determinant. After the measurement, the state ρ_X

will change to the ensemble $\{\rho_i, p_i\}$, where

$$\rho_i := \frac{1}{p_i}(I \otimes B_i)\rho_X(I \otimes B_i), \quad (12)$$

and $p_i = \text{tr}[(I \otimes B_i)\rho_X(I \otimes B_i)]$. The $\{\rho_i, p_i\}$, with $i = 0, 1$, are of subsystem A and thus 2×2 density matrices.

We may write any $V \in SU(2)$ as

$$V = tI + i\vec{y} \cdot \vec{\sigma}, \quad (13)$$

with $t, y_1, y_2, y_3 \in \mathbb{R}$ and $t^2 + y_1^2 + y_2^2 + y_3^2 = 1$. This implies that these parameters, three among them independent, assume their values in the interval $[-1, 1]$, that is, $t, y_i \in [-1, 1]$ for $i = 1, 2, 3$. The ensemble $\{\rho_i, p_i\}$ can be characterized by their eigenvalues as per a derivation given in the Appendix. The two eigenvalues each of ρ_0 and ρ_1 are given as

$$\begin{aligned} v_{\pm}(\rho_0) &= \frac{1}{2}(1 \pm \theta), \\ w_{\pm}(\rho_1) &= \frac{1}{2}(1 \pm \theta'). \end{aligned} \quad (14)$$

The corresponding probabilities are given as

$$\begin{aligned} p_0 &= [(\rho_{11} + \rho_{33})k + (\rho_{22} + \rho_{44})l], \\ p_1 &= [(\rho_{11} + \rho_{33})l + (\rho_{22} + \rho_{44})k]. \end{aligned} \quad (15)$$

We have defined θ and θ' that generalize a single expression in Ref. [15] as

$$\theta = \sqrt{\frac{[(\rho_{11} - \rho_{33})k + (\rho_{22} - \rho_{44})l]^2 + \Theta}{[(\rho_{11} + \rho_{33})k + (\rho_{22} + \rho_{44})l]^2}}, \quad (16)$$

$$\theta' = \sqrt{\frac{[(\rho_{11} - \rho_{33})l + (\rho_{22} - \rho_{44})k]^2 + \Theta}{[(\rho_{11} + \rho_{33})l + (\rho_{22} + \rho_{44})k]^2}}, \quad (17)$$

where $\Theta = 4kl[|\rho_{14}|^2 + |\rho_{23}|^2 + 2\text{Re}(\rho_{14}\rho_{23})] - 16m\text{Re}(\rho_{14}\rho_{23}) + 16n\text{Im}(\rho_{14}\rho_{23})$, and $\text{Re}(z)$ and $\text{Im}(z)$ are the real and imaginary parts of the complex number z . We have defined the parameters, m, n, k , and l as

$$\begin{aligned} m &= (ty_1 + y_2y_3)^2, \quad n = (ty_2 - y_1y_3)(ty_1 + y_2y_3), \\ k &= t^2 + y_3^2, \quad l = y_1^2 + y_2^2. \end{aligned} \quad (18)$$

With $k + l = 1$, Eqs. (16) and (17) for a given density matrix depend on three real parameters, k, m , and n . It can be readily checked that $k \in [0, 1]$, $m \in [0, 1/4]$, and $n \in [-1/8, 1/8]$. These three parameters are a recasting of the three independent parameters in Eq. (13) and are related to the set (z_1, z_2, z_3) of Ref. [15] through $4m = z_2^2$, $4n = -z_1z_2$, and $k - l = z_3$.

The entropies of the ensemble $\{\rho_i, p_i\}$ are given as

$$S(\rho_0) = -\frac{1-\theta}{2} \log_2 \frac{1-\theta}{2} - \frac{1+\theta}{2} \log_2 \frac{1+\theta}{2}, \quad (19)$$

$$S(\rho_1) = -\frac{1-\theta'}{2} \log_2 \frac{1-\theta'}{2} - \frac{1+\theta'}{2} \log_2 \frac{1+\theta'}{2}. \quad (20)$$

The quantum conditional entropy in Eq. (3) is given as

$$S(\rho_X|\{B_i\}) = p_0S(\rho_0) + p_1S(\rho_1). \quad (21)$$

As per Eq. (5), the classical correlation is obtained as

$$\begin{aligned} C(\rho_X) &= \sup_{\{B_i\}} [\mathcal{I}(\rho_X|\{B_i\})] \\ &= S(\rho_X^A) - \min_{\{B_i\}} [S(\rho_X|\{B_i\})]. \end{aligned} \quad (22)$$

Therefore, to calculate the classical correlation and consequently quantum discord, we have to minimize the quantity $S(\rho_X|\{B_i\})$ [Eq. (21)] with respect to the von Neumann measurements.

To minimize Eq. (21) by setting equal to zero its partial derivatives with respect to k, m , and n , observe first that the expression is symmetric under the interchange of k and $l = 1 - k$. It is, therefore, an even function of $(k - l)$ and the extremum lies at $k = l = 1/2$ or at the end points $k = 0$ or $k = 1$. From the definition of these parameters in Eq. (18), the end points require $t = y_3 = 0$ or $y_1 = y_2 = 0$ and, therefore, $m = n = 0$. On the other hand, for the case $k = l = 1/2$, we have $\theta = \theta'$, and $S(\rho_0) = S(\rho_1)$ and the minimization of $S(\rho_X|\{B_i\})$ is equal to the minimization of either $S(\rho_0)$ or $S(\rho_1)$. Further, with Θ in these expressions involving m and n only linearly, extreme values are attained only at their end points: $m = 0, 1/4$ and $n = 0, \pm 1/8$. Thus, the maximum classical correlation and thereby the quantum discord can be obtained easily analytically. The Appendix shows how we may generalize to POVM to get final compact expressions that are simple extensions of the more limited von Neumann measurements, thereby yielding the same value for the maximum classical correlation and discord.

For the special case of two-qubit X states with restrictions $\rho_{11} = \rho_{44}$ and $\rho_{22} = \rho_{33}$, and with real off-diagonal elements, we define

$$\begin{aligned} \theta_1 &= 2|\rho_{14} + \rho_{23}|, \quad \theta_2 = 2|\rho_{14} - \rho_{23}|, \\ \theta_3 &= \theta_4 = |(\rho_{11} + \rho_{44}) - (\rho_{22} + \rho_{33})|, \end{aligned} \quad (23)$$

and associated entropy $S'(\rho_i)|_{\theta_j}$ as

$$S'(\rho_i)|_{\theta_j} = -\frac{1+\theta_j}{2} \log_2 \frac{1+\theta_j}{2} - \frac{1-\theta_j}{2} \log_2 \frac{1-\theta_j}{2}. \quad (24)$$

In addition, $S(\rho_0) = S(\rho_1)$, and the minimum value of $S(\rho|\{B_i\})$ is equal to the minimum value of $S(\rho_0)$, which is given as

$$\min[S(\rho|\{B_i\})] = \min[S(\rho_0)] = S'(\rho_0)|_{\theta_{\text{sup}}}, \quad (25)$$

where

$$\theta_{\text{sup}} = \max\{\theta_1, \theta_2, \theta_3\}. \quad (26)$$

Therefore, we recover the results of Ref. [15] as a special case of ours. All other previous results [21] are special cases of our study and can be easily recovered.

III. RELATION BETWEEN DISCORD AND ENTANGLEMENT

In this section, we study the relation between the classical correlation, quantum discord, and entanglement for various initial states.

(1) As a first example, we take maximally entangled pure states, that is, the four Bell states given as $|\psi^{\pm}\rangle = (|0, 1\rangle \pm |1, 0\rangle)/\sqrt{2}$ and $|\phi^{\pm}\rangle = (|0, 0\rangle \pm |1, 1\rangle)/\sqrt{2}$. It is well known that for any Bell state, we have

$$\mathcal{I}(\rho) = 2, \quad C(\rho) = 1, \quad Q(\rho) = 1. \quad (27)$$

For this particular case, quantum discord and any measure of entanglement coincide and are equal to the maximum value of the correlation. Surprisingly, if we mix any two Bell states, for example, $\rho = a|\psi^+\rangle\langle\psi^+| + (1-a)|\phi^+\rangle\langle\phi^+|$, the classical correlation is not affected at all, and quantum discord is captured by a measure of entanglement called the entanglement of formation [29,30]. The quantum mutual information is $\mathcal{I}(\rho) = 2 + a \log_2 a + (1-a) \log_2(1-a)$, the classical correlation is $\mathcal{C}(\rho) = 1$, and the entanglement of formation is equal to quantum discord, that is, $\mathcal{E}(\rho) = \mathcal{Q}(\rho) = 1 + a \log_2 a + (1-a) \log_2(1-a)$ [14]. However, this example is special as, for other mixed states, entanglement and quantum discord differ substantially.

(2) We take the class of states defined as $\rho = a|\psi^+\rangle\langle\psi^+| + (1-a)|1,1\rangle\langle 1,1|$ ($0 \leq a \leq 1$), where $|\psi^+\rangle = (|0,1\rangle + |1,0\rangle)/\sqrt{2}$ is a maximally entangled state. Based on the results of the previous section, we are now able to calculate the classical correlation and quantum discord. We have $\theta_1 = \theta_2 = \sqrt{a^2 + (1-a)^2}$, $\theta_3 = |2 - 3a|/(2-a)$, and $\theta_4 = 1$. As $\theta_3 \neq \theta_4$, the quantity $S(\rho|\{B_i\})|_{\theta_3, \theta_4}$ is given as

$$S(\rho|\{B_i\})|_{\theta_3, \theta_4} = \frac{2-a}{2} S'(\rho_0)|_{\theta_3} + \frac{a}{2} S'(\rho_1)|_{\theta_4}. \quad (28)$$

As $\theta_4 = 1$, we have $S'(\rho_1)|_{\theta_4} = 0$. We note that $S'(\rho_0)|_{\theta_1} \leq S(\rho|\{B_i\})|_{\theta_3, \theta_4}$, that is, $\min\{S'(\rho_0)|_{\theta_1}, S(\rho|\{B_i\})|_{\theta_3, \theta_4}\} = S'(\rho_0)|_{\theta_1}$.

The classical correlation is given as

$$\mathcal{C}(\rho) = S(\rho^A) - S'(\rho_0)|_{\theta_1}, \quad (29)$$

where

$$S(\rho^A) = -\frac{a}{2} \log_2 \frac{a}{2} - \frac{2-a}{2} \log_2 \frac{2-a}{2}. \quad (30)$$

The quantum mutual information is

$$\mathcal{I}(\rho) = 2S(\rho^A) - S(\rho), \quad (31)$$

and the quantum discord is

$$\mathcal{Q}(\rho) = S(\rho^A) + S'(\rho_0)|_{\theta_1} - S(\rho), \quad (32)$$

where

$$S(\rho) = -a \log_2 a - (1-a) \log_2(1-a). \quad (33)$$

To study the relation between quantum discord and entanglement, we choose a measure of entanglement. Although various measures of entanglement [29–31] give the same result for separable states and for Bell states, the amount of entanglement of a specific mixed state is different for different measures. We prefer to compare quantum discord with concurrence C' [30]. The concurrence for this state is given as

$$C'(\rho) = a. \quad (34)$$

Figure 1 displays the classical correlation, quantum discord, and concurrence for ρ for various values of the parameter a . The solid line presents quantum discord, the dotted-dashed line is for concurrence, and the dashed line is for classical correlation. It can be seen that for this particular initial state, quantum discord is always less than concurrence but always greater than the classical correlation.

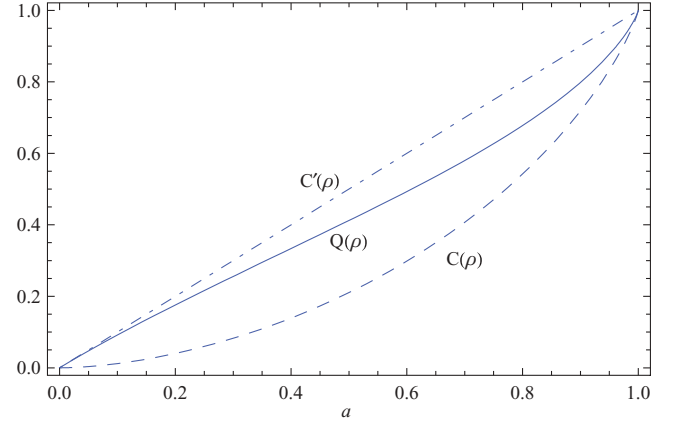


FIG. 1. (Color online) Concurrence, quantum discord, and classical correlation for the class of states in (2) under Sec. III are plotted for ρ as a function of the parameter a . These correlations are equal only for $a = 0$ and $a = 1$.

(3) We consider the initial state $\rho = a|\phi^+\rangle\langle\phi^+| + (1-a)|1,1\rangle\langle 1,1|$ ($0 < a \leq 1$), where $|\phi^+\rangle = (|0,0\rangle + |1,1\rangle)/\sqrt{2}$ is a maximally entangled state. In this case $\theta_1 = \theta_2 = \sqrt{a^2 + (a-1)^2}$, and $\theta_3 = \theta_4 = 1$. Therefore, $S(\rho|\{B_i\})|_{\theta_3, \theta_4} = 0$, which is the minimum when compared with $S'(\rho_0)|_{\theta_1}$, that is, $\min\{S'(\rho_0)|_{\theta_1}, S(\rho|\{B_i\})|_{\theta_3, \theta_4}\} = 0$. Hence the classical correlation is given as

$$\mathcal{C}(\rho) = S(\rho^A) = -\frac{a}{2} \log_2 \frac{a}{2} - \frac{2-a}{2} \log_2 \frac{2-a}{2}. \quad (35)$$

The quantum mutual information is given as

$$\mathcal{I}(\rho) = 2S(\rho^A) - S(\rho), \quad (36)$$

and quantum discord as

$$\mathcal{Q}(\rho) = S(\rho^A) - S(\rho), \quad (37)$$

with $S(\rho)$ as in Eq. (24). The concurrence for these states is again given as in Eq. (34), $C'(\rho) = a$.

The classical correlation, quantum discord, and concurrence have been plotted in Fig. 2 for ρ against parameter a .

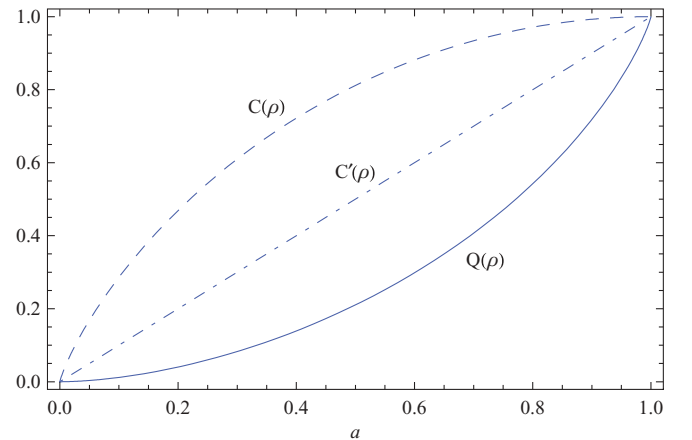


FIG. 2. (Color online) As in Fig. 1 for the class of states in (3) under Sec. III. The top curve (dashed line) is for classical correlation, the middle curve (dotted-dashed) is for concurrence, and the bottom curve (solid line) is for quantum discord.

The solid line is for quantum discord, the dotted-dashed line is for concurrence, and the dashed line is for classical correlation. Interestingly, for this particular initial state, the classical correlation is always greater than both entanglement and quantum discord except for $a = 0$ and $a = 1$. Moreover, quantum discord is always less than concurrence and the classical correlation.

(4) Let us consider the Werner state [25],

$$\rho = a|\psi^-\rangle\langle\psi^-| + \frac{1-a}{4}I, \quad (38)$$

where $|\psi^-\rangle = (|0,1\rangle - |1,0\rangle)/\sqrt{2}$ is a maximally entangled state and $0 \leq a \leq 1$. The Werner state has a peculiar property in that the eigenvalues of its ensemble $\{p_i, \rho_i\}$ do not depend on the parameters k and m , that is, $\theta = \theta' = a$ or in other words $\theta_1 = \theta_2 = \theta_3 = a$, and we have [15]

$$\mathcal{C}(\rho) = \frac{1-a}{2} \log_2(1-a) + \frac{1+a}{2} \log_2(1+a), \quad (39)$$

$$\mathcal{I}(\rho) = \frac{3(1-a)}{4} \log_2(1-a) + \frac{1+3a}{4} \log_2(1+3a), \quad (40)$$

and quantum discord

$$\begin{aligned} \mathcal{Q}(\rho) &= \mathcal{I}(\rho) - \mathcal{C}(\rho) \\ &= \frac{1}{4}[(1-a) \log_2(1-a) + (1+3a) \log_2(1+3a) \\ &\quad - 2(1+a) \log_2(1+a)]. \end{aligned} \quad (41)$$

The concurrence for the Werner state is given by

$$C'(\rho) = \max \left\{ 0, \frac{3a-1}{2} \right\}. \quad (42)$$

These correlations are plotted in Fig. 3. In contrast to previous examples, the correlations have a different order as functions of a , with quantum discord initially larger than concurrence and the classical correlation for $0 \leq a \lesssim 0.523$, but for the range $0.523 < a < 1$, concurrence becomes larger than discord and the classical correlation. Such a behavior is different from the previous two examples.

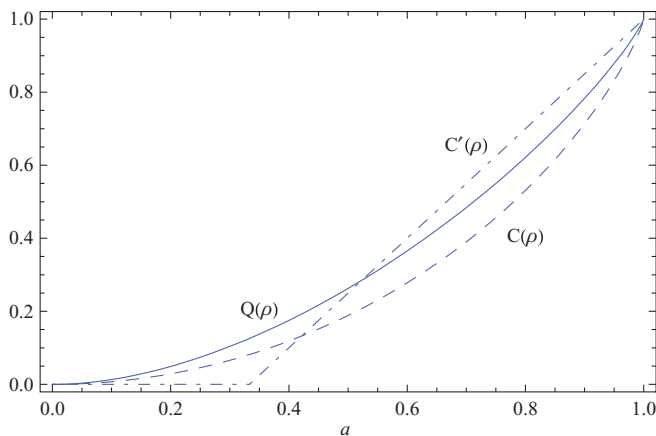


FIG. 3. (Color online) Graphs of quantum discord $\mathcal{Q}(\rho)$ (solid line), classical correlation $\mathcal{C}(\rho)$ (dashed line), and concurrence $C'(\rho)$ (dotted-dashed line) versus a for the Werner state.

(5) Finally we consider the initial state,

$$\rho = \frac{1}{3}\{(1-a)|0,0\rangle\langle 0,0| + 2|\psi^+\rangle\langle\psi^+| + a|1,1\rangle\langle 1,1|\}. \quad (43)$$

In contrast with example (2), this state also contains the $|0,0\rangle$ noisy component. We note that $\theta_1 = \theta_2 = \sqrt{(1-2a)^2 + 4}/3$, $\theta_3 = (1-a)/(1+a)$, and $\theta_4 = a/(2-a)$. We find $S'(\rho_0)|_{\theta_1} < S(\rho|\{B_i\})|_{\theta_3, \theta_4}$, that is, $\min\{S'(\rho_0)|_{\theta_1}, S(\rho|\{B_i\})|_{\theta_3, \theta_4}\} = S'(\rho_0)|_{\theta_1}$. We have

$$\begin{aligned} \mathcal{C}(\rho) &= \frac{1+\theta_1}{2} \log_2 \frac{1+\theta_1}{2} + \frac{1-\theta_1}{2} \log_2 \frac{1-\theta_1}{2} \\ &\quad - \frac{2-a}{3} \log_2 \frac{2-a}{3} - \frac{1+a}{3} \log_2 \frac{1+a}{3}, \end{aligned} \quad (44)$$

$$\begin{aligned} \mathcal{I}(\rho) &= \frac{1-a}{3} \log_2 \frac{1-a}{3} + \frac{a}{3} \log_2 \frac{a}{3} + \frac{2}{3} \log_2 \frac{2}{3} \\ &\quad - \frac{2(2-a)}{3} \log_2 \frac{2-a}{3} - \frac{2(1+a)}{3} \log_2 \frac{1+a}{3}, \end{aligned} \quad (45)$$

and quantum discord

$$\begin{aligned} \mathcal{Q}(\rho) &= \frac{1-a}{3} \log_2 \frac{1-a}{3} + \frac{a}{3} \log_2 \frac{a}{3} + \frac{2}{3} \log_2 \frac{2}{3} \\ &\quad - \frac{(2-a)}{3} \log_2 \frac{2-a}{3} - \frac{(1+a)}{3} \log_2 \frac{1+a}{3} \\ &\quad - \frac{1+\theta_1}{2} \log_2 \frac{1+\theta_1}{2} - \frac{1-\theta_1}{2} \log_2 \frac{1-\theta_1}{2}. \end{aligned} \quad (46)$$

The concurrence for this state is given as

$$C'(\rho) = \max \left\{ 0, \frac{2}{3}[1 - \sqrt{a(1-a)}] \right\}. \quad (47)$$

We display the classical correlation, quantum discord, and concurrence versus a for this state in Fig. 4. We can see that all these correlations are symmetric about $a = 1/2$. As the parameter a varies from 0 to 1, the quantum mutual information decreases, and the classical correlation, quantum discord, and entanglement decrease, and vice versa.

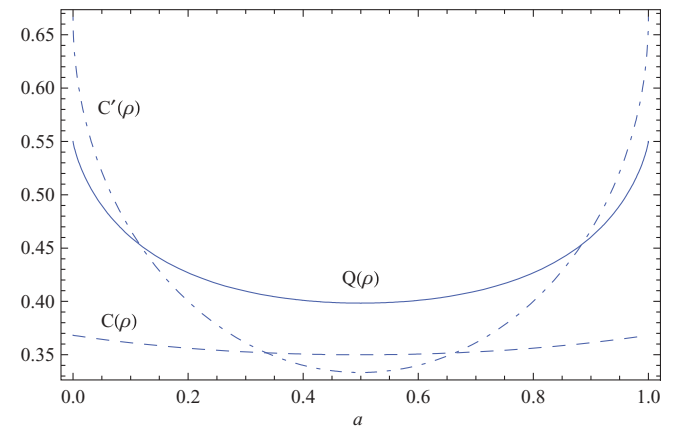


FIG. 4. (Color online) Graphs of quantum discord $\mathcal{Q}(\rho)$ (solid line), classical correlation $\mathcal{C}(\rho)$ (dashed line), and concurrence $C'(\rho)$ (dotted-dashed line) versus a . The correlations are symmetrical about $a = 0.5$ and are maximum at $a = 0$ and $a = 1$.

IV. SUMMARY

We have derived analytical expressions for the classical correlation and quantum discord in X states, a seven-parameter family of states of two qubits. This generalizes results previously available only for a three-parameter subset of such states. A large class of two-qubit states that includes maximally or partially entangled states and mixed states that are separable or nonseparable can now be examined for these various correlations. We present such results for the classical correlation, quantum discord, and entanglement for various density matrices. We conclude that there are no simple ordering relations between these correlations and, in particular, that quantum discord may be smaller or larger than entanglement as measured with concurrence or negativity. Thus, quantum discord is a fundamentally different resource than entanglement and these correlations are different qualitatively and quantitatively.

ACKNOWLEDGMENTS

We thank Drs. Jaroslav Novotný and Joseph Rennes for discussions. M.A. would like to thank Professor Christof Wunderlich for his kind hospitality at the Universität Siegen where part of this work is done. M.A. acknowledges financial support by the Higher Education Commission, Pakistan, and by the DAAD. A.R.P.R. acknowledges support from the Alexander von Humboldt Foundation.

APPENDIX: CALCULATIONAL DETAILS OF VON NEUMANN AND POVM ALTERNATIVES

In this appendix, we give some details of the calculation leading to Eqs. (15)–(20). First, an alternative seven-parameter version of the density matrix in Eq. (7) proves useful:

$$\rho_X = \frac{1}{4} \begin{pmatrix} 1+d_1 & 0 & 0 & c_1-c_2 \\ 0 & 1+d_2 & c_1+c_2 & 0 \\ 0 & c_1^*+c_2^* & 1+d_3 & 0 \\ c_1^*-c_2^* & 0 & 0 & 1+d_4 \end{pmatrix}, \quad (\text{A1})$$

where c_1 and c_2 are complex and the other coefficients are real, the diagonal entries being ($d_1 = c_3 + a_3 + b + 3$, $d_2 = -c_3 + a_3 - b_3$, $d_3 = -c_3 - a_3 + b_3$, $d_4 = c_3 - a_3 - b_3$). These parameters are given in terms of the density matrix elements by $c_3 = \rho_{11} + \rho_{44} - \rho_{22} - \rho_{33}$, $a_3 = \rho_{11} - \rho_{44} + \rho_{22} - \rho_{33}$, $b_3 = \rho_{11} - \rho_{44} - \rho_{22} + \rho_{33}$, $c_1 = 2(\rho_{23} + \rho_{14})$, and $c_2 = 2(\rho_{23} - \rho_{14})$. The choice of only three coefficients c_i , all real, corresponds to the one made in Ref. [15].

Evaluation of Eq. (12) as per the procedure in Ref. [15] gives, after some algebra,

$$\begin{aligned} p_0 \rho_0 &= \frac{1}{4} [1 + b_3 z_3 + a_1 \sigma_1 + a_2 \sigma_2 + (a_3 + c_3 z_3) \sigma_3], \\ p_1 \rho_1 &= \frac{1}{4} [1 - b_3 z_3 - a_1 \sigma_1 - a_2 \sigma_2 + (a_3 - c_3 z_3) \sigma_3], \end{aligned} \quad (\text{A2})$$

with

$$\begin{aligned} a_1 &= \text{Re}(z_1 c_1 - i z_2 c_2) = z_1 \text{Re}(c_1) + z_2 \text{Im}(c_2), \\ a_2 &= \text{Im}(z_1 c_1 - i z_2 c_2) = z_2 \text{Re}(c_2) - z_1 \text{Im}(c_1), \end{aligned} \quad (\text{A3})$$

in terms of the unit vector \vec{z} defined in Ref. [15] from the parameters in Eq. (13) as

$$\begin{aligned} z_1 &= 2(-t y_2 + y_1 y_3), & z_2 &= 2(t y_1 + y_2 y_3), \\ z_3 &= t^2 + y_3^2 - y_1^2 - y_2^2. \end{aligned} \quad (\text{A4})$$

Upon taking the trace of Eq. (A2), we get the probabilities

$$p_0 = (1 + b_3 z_3)/2, \quad p_1 = (1 - b_3 z_3)/2, \quad (\text{A5})$$

in agreement with Eq. (15) upon writing b_3 in terms of ρ_{ij} and $z_3 = k - l$.

The density matrices themselves for subsystem A that follow from Eq. (A2) are, therefore,

$$\begin{aligned} \rho_0 &= \frac{1}{2} \{I + [a_1 \sigma_1 + a_2 \sigma_2 + (a_3 + c_3 z_3) \sigma_3] / (1 + b_3 z_3)\}, \\ \rho_1 &= \frac{1}{2} \{I + [-a_1 \sigma_1 - a_2 \sigma_2 + (a_3 - c_3 z_3) \sigma_3] / (1 - b_3 z_3)\}. \end{aligned} \quad (\text{A6})$$

Their eigenvalues are the ones in Eq. (14). Note that the denominators in Eq. (17) are $(1 \pm b_3 z_3)/2$, while the numerators under the square root are the sum of the squares of $(a_3 \pm c_3 z_3)/2$ and $\Theta = (a_1^2 + a_2^2)/4$ as follows from the properties of the Pauli matrices. The expressions for ρ_0 and ρ_1 differ in a change in sign in \vec{z} in Eqs. (A6) and (A3). This close connection except for a change in sign of \vec{z} traces back to the similar change in sign of the two von Neumann projectors in Eq. (11), $\Pi_{0,1} = (I \pm \sigma_z)/2$. Indeed, the reduction of the lengthy calculation to this compact statement of passing from the projectors $\Pi_{0,1}$ to the expressions in Eq. (A6), with the measurement directions $\pm \hat{z}$ replaced by the dot product of $\vec{\sigma}$ with \vec{z} and corresponding coefficients of the density matrix, will be useful in generalizing to other types of measurements below.

Instead of von Neumann projectors, consider more general POVM. For instance, choose three orthogonal unit vectors mutually at 120° ,

$$\hat{s}_{0,1,2} = [\hat{z}, (-\hat{z} \pm \sqrt{3}\hat{x})/2], \quad (\text{A7})$$

and corresponding projectors

$$E_0 = \frac{1}{3}(I + \sigma_z), \quad (\text{A8})$$

$$E_{1,2} = \frac{1}{3} \left(I - \frac{1}{2} \sigma_z \pm \frac{\sqrt{3}}{2} \sigma_x \right),$$

with $E_0 + E_1 + E_2 = I$, $E_i^2 = 2E_i/3$, and $\text{tr}(E_i) = 2/3$. With this choice of projectors in Eq. (11), the same calculation for what remains for subsystem A after the measurements on subsystem B now give the counterparts of Eq. (A5),

$$\begin{aligned} p_0 &= (1 + b_3 z_3)/3, & p_1 &= (1 + b_3 \alpha_3)/2, \\ p_2 &= (1 + b_3 \beta_3)/3, \end{aligned} \quad (\text{A9})$$

and of Eq. (A6) for $\rho_{0,1,2}$ with exactly similar expressions except $(\vec{z}, \vec{\alpha}, \vec{\beta})$ replaces $\pm \vec{z}$ in Eqs. (A6) and (A3). Here, we have defined two counterparts of \vec{z} that follow from the other two projectors in Eq. (A7),

$$\vec{\alpha}, \vec{\beta} = (-\vec{z} \pm \sqrt{3}\vec{x})/2, \quad (\text{A10})$$

with \vec{z} given in Eq. (A4) in terms of the parameters in Eq. (13), and similarly we have defined \vec{x} drawn from another set of

combinations in Ref. [15],

$$\begin{aligned} x_1 &= t^2 + y_1^2 - y_2^2 - y_3^2, & x_2 &= 2(-ty_3 + y_1y_2), \\ x_3 &= 2(ty_2 + y_1y_3). \end{aligned} \quad (\text{A11})$$

Other choices of projectors may define a similar third set of parameters \vec{y} in Ref. [15], all these unit vectors $(\vec{x}, \vec{y}, \vec{z})$ being mutually orthogonal.

-
- [1] G. Alber, T. Beth, M. Horodecki, P. Horodecki, R. Horodecki, M. Rötteler, H. Weinfurter, R. Werner, and A. Zeilinger, *Quantum Information* (Springer-Verlag, Berlin, 2001), Chap. 5.
- [2] R. Horodecki, P. Horodecki, M. Horodecki, and K. Horodecki, *Rev. Mod. Phys.* **81**, 865 (2009).
- [3] M. A. Nielsen and I. L. Chuang, *Quantum Computation and Quantum Information* (Cambridge University Press, Cambridge, UK, 2000).
- [4] C. H. Bennett, D. P. DiVincenzo, C. A. Fuchs, T. Mor, E. Rains, P. W. Shor, J. A. Smolin, and W. K. Wootters, *Phys. Rev. A* **59**, 1070 (1999).
- [5] M. Horodecki, P. Horodecki, R. Horodecki, J. Oppenheim, A. Sen, U. Sen, and B. Synak-Radtke, *Phys. Rev. A* **71**, 062307 (2005).
- [6] J. Niset and N. J. Cerf, *Phys. Rev. A* **74**, 052103 (2006).
- [7] S. L. Braunstein, C. M. Caves, R. Jozsa, N. Linden, S. Popescu, and R. Schack, *Phys. Rev. Lett.* **83**, 1054 (1999).
- [8] D. A. Meyer, *Phys. Rev. Lett.* **85**, 2014 (2000).
- [9] A. Datta, S. T. Flammia, and C. M. Caves, *Phys. Rev. A* **72**, 042316 (2005); A. Datta and G. Vidal, *ibid.* **75**, 042310 (2007); A. Datta, A. Shaji, and C. M. Caves, *Phys. Rev. Lett.* **100**, 050502 (2008).
- [10] B. P. Lanyon, M. Barbieri, M. P. Almeida, and A. G. White, *Phys. Rev. Lett.* **101**, 200501 (2008).
- [11] B. Groisman, S. Popescu, and A. Winter, *Phys. Rev. A* **72**, 032317 (2005).
- [12] B. Schumacher and M. D. Westmoreland, *Phys. Rev. A* **74**, 042305 (2006).
- [13] H. Ollivier and W. H. Zurek, *Phys. Rev. Lett.* **88**, 017901 (2001).
- [14] L. Henderson and V. Vedral, *J. Phys. A* **34**, 6899 (2001); V. Vedral, *Phys. Rev. Lett.* **90**, 050401 (2003); J. Maziero, L. C. Celéri, R. M. Serra, and V. Vedral, *Phys. Rev. A* **80**, 044102 (2009).
- [15] S. Luo, *Phys. Rev. A* **77**, 042303 (2008).
- [16] N. Li and S. Luo, *Phys. Rev. A* **76**, 032327 (2007); S. Luo, *ibid.* **77**, 022301 (2008).
- [17] J. Oppenheim, M. Horodecki, P. Horodecki, and R. Horodecki, *Phys. Rev. Lett.* **89**, 180402 (2002).
- [18] D. Kaszlikowski, A. Sen(De), U. Sen, V. Vedral, and A. Winter, *Phys. Rev. Lett.* **101**, 070502 (2008).
- [19] R. Dillenschneider, *Phys. Rev. B* **78**, 224413 (2008).
- [20] M. S. Sarandy, *Phys. Rev. A* **80**, 022108 (2009).
- [21] J. Maziero, T. Werlang, F. F. Fanchini, L. C. Céleri, and R. M. Serra, *Phys. Rev. A* **81**, 022116 (2010); F. F. Fanchini, T. Werlang, C. A. Brasil, L. G. E. Arruda, and A. O. Caldeira, e-print [arXiv:0911.1096](https://arxiv.org/abs/0911.1096) [quant-ph].
- [22] J. Maziero, H. C. Guzman, L. C. Céleri, M. S. Sarandy, and R. M. Serra, e-print [arXiv:1002.3906](https://arxiv.org/abs/1002.3906) [quant-ph]; L. Mazzola, J. Piilo, and S. Maniscalco, e-print [arXiv:1001.5441](https://arxiv.org/abs/1001.5441) [quant-ph].
- [23] A. R. Usha Devi and A. K. Rajagopal, *Phys. Rev. Lett.* **100**, 140502 (2008).
- [24] T. Werlang, S. Souza, F. F. Fanchini, and C. J. Villas Boas, *Phys. Rev. A* **80**, 024103 (2009).
- [25] R. F. Werner, *Phys. Rev. A* **40**, 4277 (1989).
- [26] T. Yu and J. H. Eberly, *Quantum Inform. Comput.* **7**, 459 (2007).
- [27] A. R. P. Rau, *J. Phys. A* **42**, 412002 (2009).
- [28] A. Sanpera, R. Tarrach, and G. Vidal, *Phys. Rev. A* **58**, 826 (1998).
- [29] C. H. Bennett, D. P. DiVincenzo, J. A. Smolin, and W. K. Wootters, *Phys. Rev. A* **54**, 3824 (1996).
- [30] W. K. Wootters, *Phys. Rev. Lett.* **80**, 2245 (1998).
- [31] G. Vidal and R. F. Werner, *Phys. Rev. A* **65**, 032314 (2002).